

Intercomparison of normalized head-scatter factor measurement techniques^{a)}

Douglas M. D. Frye,^{b)} Bhudatt R. Paliwal, Bruce R. Thomadsen, and Paul Jursinic^{c)}
University of Wisconsin Hospital, Madison, Wisconsin

(Received 11 December 1993; accepted for publication 22 November 1994)

Normalized head-scatter factors were measured with cylindrical beam coaxial miniphantoms and high purity graphite buildup caps for 4-, 6-, 10-, and 24-MV photon beams at field sizes from 4×4 to 40×40 cm². The normalized head-scatter factors determined by the two methods matched well for 4- and 6-MV photon beams. The miniphantom technique produced normalized head-scatter factors 1.5% and 4.8% lower than the buildup caps for the 10- and 24-MV beams for large field sizes, respectively. At small field sizes, the miniphantom technique produced larger normalized head-scatter factors than the buildup caps. Measurements made with an electromagnet indicate that a significant portion of the ionization measured in the buildup cap at 24 MV arises from contamination electrons. Measurements made with the miniphantom and magnet found no contamination electron contribution. The miniphantom technique may exclude such contamination electrons, potentially leading to inaccuracies in tissue-maximum ratios and phantom scatter factors, as well as inaccuracies in monitor unit calculations.

Key words: radiation therapy, dosimetry, measurement, head-scatter factor

I. INTRODUCTION

The determination of the head-scatter factor (S_c) is a key measurement in tissue-maximum ratio (TMR) dosimetry. The head-scatter factor, also termed the collimator scatter factor, is determined from the relation

$$S_c(r) = Q(r)/Q(r_0), \quad (1)$$

where $Q(r)$ is the ionization measured in air in an equilibrium mass of tissue equivalent material at field size r , and $Q(r_0)$ is the ionization measured under the same conditions except that the collimator jaws are set to the normalization field size, r_0 . Head scatter consists largely of photons and electrons arising from the field flattening filter and collimator assembly. The accuracy TMR based dosimetric calculations can be significantly influenced by the determination of S_c . The dependence of the TMR upon S_c arises from the relationship between S_c , the total scatter factor ($S_{c,p}$), and the phantom scatter factor (S_p)

$$S_p(r) = S_{c,p}(r)/S_c(r). \quad (2)$$

Determination of the TMR from percentage depth dose (PDD) and the scatter-maximum (SMR) from TMR are dependent upon accurate S_p values under the relation

$$\text{TMR}(d, r_d) = \frac{P(d, r, f)}{100} \left(\frac{f+d}{f+t_0} \right)^2 \left(\frac{S_p(r_{t_0})}{S_p(r_d)} \right), \quad (3)$$

where r , r_{t_0} , and r_d are the field sizes at f , $f+t_0$, and $f+d$, as described by Khan.¹

Inaccuracies introduced in the measurement of S_c values could influence the TMR values determined using them through Eq. (2). In addition, monitor unit calculations directly utilize measured head-scatter factors through the relation

$$\text{MU} = \frac{\dot{D}_0}{\text{TMR}(r_d, d) S_c(r_c) S_p(r_d) \text{WF TF}}, \quad (4)$$

where MU is the number of monitor units, \dot{D}_0 is the dose per monitor unit at isocenter, $\text{TMR}(r_d, d)$ is the tissue-maximum ratio for field size r_d at depth d , $S_c(r_c)$ is the head-scatter factor for the collimator setting r_c , $S_p(r_d)$ is the phantom scatter factor for field size r_d determined from Eq. (1), WF is the wedge factor, and TF is the tray factor. Inaccurate monitor unit values could result from calculations using erroneous S_c values obtained through inappropriate measurement techniques.

Beam coaxial cylindrical miniphantoms have been employed by several investigators for determination of head-scatter factors.²⁻⁴ Other investigators have employed conventional buildup caps of varying composition and thickness to determine these factors.⁵⁻⁷ The large thicknesses used in the miniphantom measurement technique differ substantially from the buildup cap thicknesses conventionally employed for head-scatter measurements. The greater thicknesses of the miniphantoms are intended to convey the following advantages: elimination of contamination electrons, congruence with European dosimetry protocols, the measurement of information in a region more relevant to clinical interest, independence from variation of d_{max} with field size, and avoidance of the problems associated with high atomic number buildup caps.³ The current investigation sought to compare the normalized head-scatter factors obtained with both techniques, explore the source of any differences, and discuss the clinical relevance of any differences.

II. MATERIALS AND METHODS

Illustrations depicting the miniphantoms and buildup caps employed in the current investigation are shown in Fig. 1. The miniphantoms were constructed of RMI Solid WaterTM. The buildup caps were made of high purity graphite with equilibrium thickness (d_{max}) walls, listed in Table I.⁸ Miniphantom measurements employed a 0.6 cc PTW model N23333 Farmer chamber with a Keithley model 602 electrometer and Fluke model 8060A digital multi-meter (DMM). The buildup

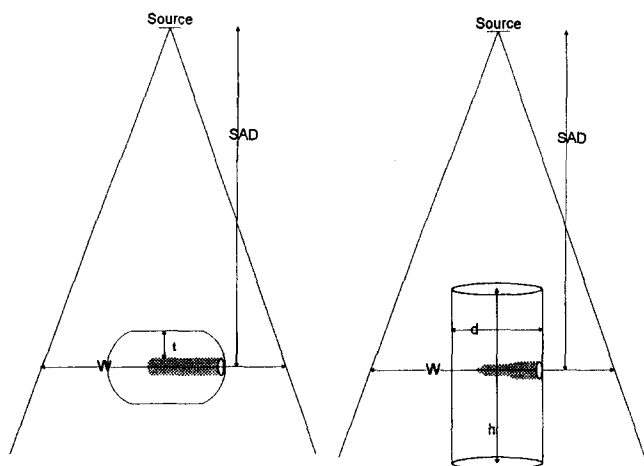


FIG. 1. Normalized head-scatter factor measurement irradiation geometry, where h is the miniphantom thickness, d is the miniphantom diameter, and t is the buildup cap thickness. In all miniphantom measurements the measurement depth was one-half the phantom thickness. A Scanditronix model RK 0.1 cc ionization chamber was employed in the buildup caps and a PTW model N23333 0.6 cc Farmer ionization chamber was used in the miniphantoms. Subsequent measurements using the Farmer chamber in the buildup caps demonstrated no significant difference between results obtained with the two different chambers.

cap measurements used a Scanditronix model RK 0.1 cc ionization chamber and Precision Radiation Measurements (PRM) model SH1 electrometer. Subsequent measurements using the Farmer chamber in the buildup caps at selected field sizes (7×7 , 10×10 , 15×15 , and 20×20 cm²) instead of the Scanditronix chamber demonstrated no significant difference between results obtained with the different ion chambers. Both electrometers had current National Institute of Standards and Technology (NIST) traceable calibrations. The ion chambers were tested for stem effect. Stem effects were measured by irradiation of the chambers' stems with elongated fields in which the long axis of the fields were placed parallel and perpendicular to the ion chamber stems, as described in National Council on Radiation Protection and Measurements (NCRP) report 69. Stem effect measurements were performed on a Clinac 4 with no buildup cap or miniphantom at 80-cm source to chamber distance (SCD) with a 5×28 cm² field size. No stem effects were detected.

Normalized head-scatter factors (S_c) were measured on Varian Clinac 4, 2100c, and 2500 accelerators for 4-, 6-, 10-, and 24-MV photon beams. The irradiation geometries are depicted in Fig. 1. Charge was accumulated for 200 monitor unit irradiations at each field size. Charge measurements were repeated at regular intervals for previously measured

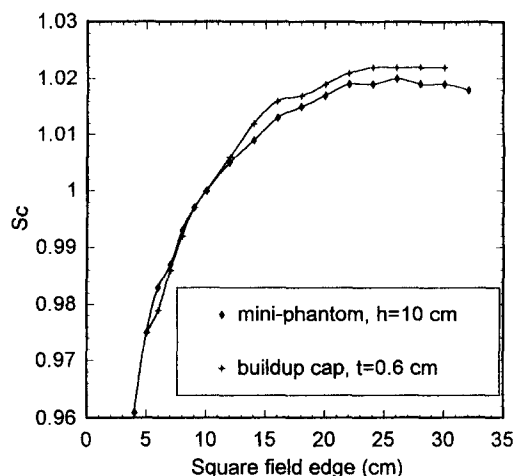


FIG. 2. Normalized head-scatter factors, 4-MV photon beam.

field sizes to detect any systematic drift in the dosimetry or accelerator systems. No such drifts were detected. Data were obtained for integer square field sizes between 4×4 and 10×10 cm², then for every even integer square field size up to the maximum field size of the unit, 32×32 cm² for the Clinac 4, and 40×40 cm² for the 2100c and 2500. Miniphantom total thicknesses (h) and buildup cap wall thicknesses employed for the measurements are given in the Table and illustrated in Fig. 1. Measurements were obtained with miniphantom thicknesses and diameters as per van Gasteren³ and also at thicknesses of twice the dose maximum depth ($h = 2 \times d_{\max}$) for the 10-MV ($d_{\max} = 2.5$ cm) and 24-MV ($d_{\max} = 4$ cm) photon beams. In all miniphantom measurements the measurement depth was one-half the phantom thickness.

The effects of contamination electrons upon normalized head-scatter factor measurements at 10- and 24-MV photon energies were also investigated. Charge was measured with the buildup cap technique for various field sizes at various SCDs. Charge measurements were also obtained with the buildup caps and miniphantoms for a 10×10 cm² field at various SCDs with the radiation beam passing through a magnetic field directed perpendicularly to the central axis. The magnet employed was a combination permanent/electromagnet. Reduced field strengths could be obtained by "bucking," or opposing, the permanent magnet with the electromagnet. A 1446-G field strength was achieved by assisting the permanent magnet with the electromagnet. The magnet was designed to fit in the accessory tray holder with the pole faces parallel to the central axis. Field sizes were limited to a maximum of 10×10 cm² at isocenter due to the magnet's pole gap. The 1446-G field has been demonstrated to sweep all contamination electrons from the 24-MV photon beam.⁹ Charge measurements were obtained for the 24-MV photon beam at 0- and 1446-G field strengths with the buildup cap and miniphantom.

III. RESULTS

The measured head-scatter factors, normalized to a 10×10 cm² field size, are illustrated in Figs. 2–5. The data

TABLE. Phantom thicknesses for normalized head-scatter measurements.

Photon beam energy (MV)	Miniphantom thickness, h (cm)	Miniphantom diameter, d (cm)	Buildup cap wall thickness, t (cm)
4	10	4	0.6
6	10	4	0.9
10	5.20	4	1.3
24	8.20	4	2.3

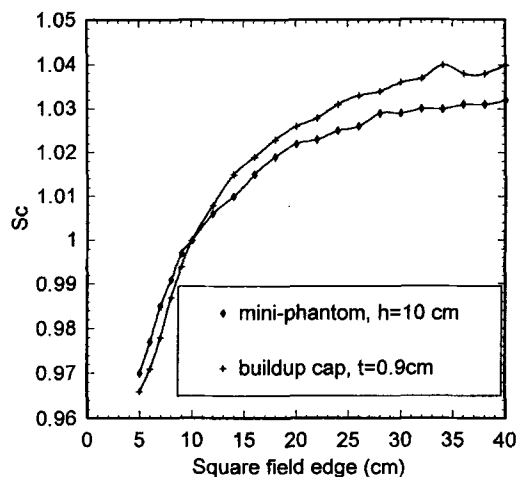


FIG. 3. Normalized head-scatter factors, 6-MV photon beam.

points in the figures have been connected by splines. The results in Figs. 2 and 3 indicate there is no significant difference (0.5%) between head-scatter factors obtained with the buildup cap and miniphantom techniques for 4- and 6-MV photon beams. The 10-MV results (Fig. 4) exhibit a 1% to 1.5% difference between the head-scatter factors determined with the buildup cap and equilibrium thickness miniphantom ($h = 2d_{\max} = 5$ cm) and those measured with the thick miniphantom ($h = 20$ cm) for field sizes between 15×15 and 40×40 cm². The head-scatter factors obtained for the 24-MV beam (Fig. 5) exhibit a substantial difference (4.8%) between the results obtained with the buildup cap and miniphantom. Note also the relative relation between the results of the two techniques reverses at field sizes below the normalization point. Measurements at 24 MV with a miniphantom thickness of twice the depth of the dose maximum ($h = 2 \times d_{\max} = 8$ cm) resulted in head-scatter factors not significantly different (0.5%) from those obtained with the buildup cap.

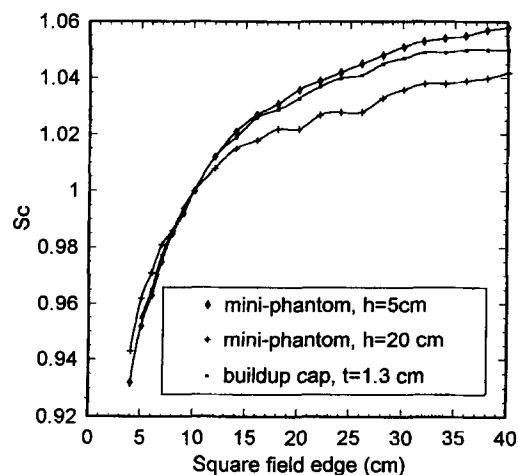


FIG. 4. Normalized head-scatter factors, 10-MV photon beam.

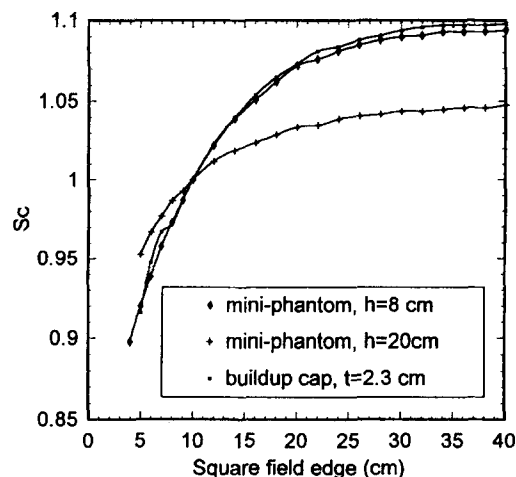


FIG. 5. Normalized head-scatter factors, 24-MV photon beam.

The investigation of contamination electrons effects in the 24-MV photon beam provided the results illustrated in Fig. 6. The results in the figure have been normalized to readings at 100-cm SCD. The persistent difference between the 0- and 1446-G results at the investigated SCDs suggest that the majority of contamination electrons have in-air ranges exceeding the SCDs investigated. The experiment was repeated with the thicker ($h = 20$ cm) miniphantom. The use of the 1446-G magnetic field to sweep contamination electrons from the beam produced no change in collected charge with the thicker miniphantom.

IV. DISCUSSION

The measurements using the magnetic field to sweep the 24-MV photon beam indicate that electrons arising from the treatment unit head represent a significant portion (3.9% for

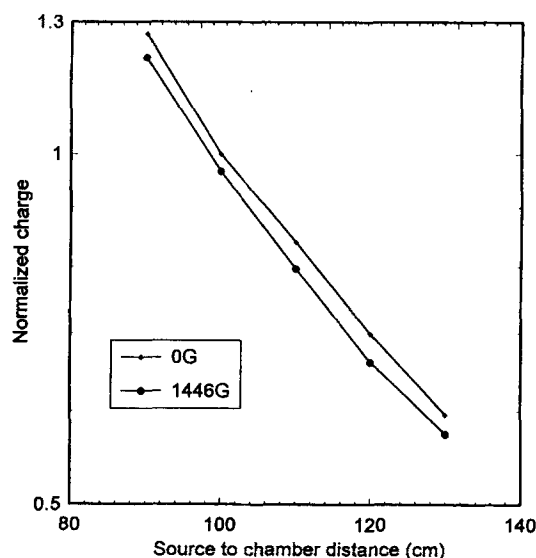


FIG. 6. Normalized charge vs source-to-chamber distance for 0- and 1446-G applied magnetic field, 24-MV photon beam, graphite buildup cap (2.3-cm wall thickness), 10×10 cm² field size. Results have been normalized to 0-G field strength and 100 cm source-to-chamber distance.

a 10×10 cm² field) of the difference between the measurements made with buildup caps and those made with the thicker miniphantoms as described by van Gasteren *et al.*³ Thomadsen *et al.* have previously demonstrated that contamination electrons for such high energy photon beams reach to and beyond the deepest value of the dose maximum depth.¹⁰ Biggs and Ling, Biggs and Russel, and Ling, Schell, and Rustgi also demonstrated that for such beams a significant portion of the dose between the surface and the dose maximum depth comes from electron contamination.^{11–13} The convergence of miniphantom and buildup cap results which occurs when miniphantoms of twice d_{\max} thickness are employed support this finding. While we have been unable to demonstrate a field size dependent electron contamination component of S_c at isocenter with our current magnet due to pole gap constraints, Thomadsen *et al.* previously found that contamination electrons contributed 0.4%, 5.3%, and 10% to the ionization at the depth of dose maximum for 10×10 , 20×20 , and 35×35 cm² fields at 205.5-cm source to detector distance in the 24-MV photon beam.¹⁰ The use of thick miniphantoms for the measurement of S_c of the highest energy photon beams, as per van Gasteren, appears to exclude such contamination electrons, which would otherwise be found at the depth of dose maximum. The results indicate that for 24-MV photon beams the thicker miniphantoms are not appropriate tools for use in S_c measurements which will be employed in a TMR dosimetry system.

The presence of a field size dependent contamination electron component of head scatter for the highest energy photon beams would be consistent with our findings. The thicker miniphantom reduces the ionization at the normalization field size in Eq. (1). If the ionization of smaller field sizes is less effected by such contamination electrons, then the normalization value would be reduced and the head-scatter factor, the ratio of ionizations, would increase for smaller field sizes, as indicated in the measurements reported here. For large field sizes, where electron contamination contributions may be significant, the exclusion of the contamination electrons would be expected to reduce the numerator of the ratio in Eq. (1) more significantly than the denominator. The resulting S_c would be reduced, as observed in the measurements reported here.

The results of the measurements reported here indicate that TMR dosimetry of the highest energy photon beams could be significantly effected by the head-scatter factor measurement technique employed. Determination of phantom scatter factors and TMR values could be influenced through the relations described in Eq. (2)–(4). Phantom scatter factor values could be overestimated (small field sizes) or underestimated (large field sizes) through Eq. (2) by use of head-scatter factors obtained from measurements using the thick miniphantoms. TMR values derived through Eq. (3) would be directly effected by these inaccuracies. Overestimates of the phantom scatter factor $S_p(r_d)$ for large field sizes would tend to overwhelm the normalization field size phantom scatter factor $[S_p(t_0)]$ in Eq. (3) and produce underestimated TMRs for large field sizes. For smaller field sizes the underestimated phantom scatters would produce overestimated TMRs.

The calculation of monitor units for the highest energy photon beams could also be effected by the choice of the head-scatter factor measurement technique. The calculation of monitor units depends directly upon the measured head-scatter factors through the relation described in Eq. (4). For open fields the problem is avoided because the product $S_c S_p$ reduces to the measured open field total scatter factor, $S_{c,p}$. However, for moderately blocked fields, the use of head-scatter factors measured with the miniphantoms in monitor unit calculations may lead to inaccuracies dependent upon the collimator field size and the degree of blocking. For example, when the field size is larger than the normalization field size of 10×10 cm², the head-scatter factor, which is underestimated by the miniphantom technique, is not completely compensated by the overestimated phantom scatter factor, since the blocked field size is inevitably smaller than the collimator setting, thereby leading to an overestimate of the necessary monitor units. If the TMRs used in the monitor unit calculation are derived from Eq. (3), as described in the preceding paragraph, the overestimate of monitor units could be compounded. For field sizes smaller than 10×10 cm² the situation is reversed, with underestimation of the number of monitor units.

In summary, the measurements described above indicate that the miniphantom technique for measuring head-scatter factors, as described by van Gasteren *et al.*,³ may lead to inaccuracies in TMR dosimetry for 24-MV photon fields. Measurements with a 1446-G electromagnet indicate that a significant portion of the total ionization normally measured with conventional buildup cap techniques at the depth of maximum dose in the 24-MV photon beam is due to contamination electrons, and that the contributions of these electrons are excluded by the miniphantom thicknesses described by van Gasteren *et al.*³ Previous work by Thomadsen *et al.* indicate a field size dependent electron contamination component of head scatter.¹⁰ The results of our measurements demonstrate that for such high energy photon beams inaccuracy may result if the headscatter measurement technique fails to match the secondary charged particle environment at depth of the normalization for the dosimetry system.

^aPresented at the 1993 Annual Meeting (Spring) of the North Central Chapter of the AAPM.

^bPresent address: MetroHealth Medical Center, Case Western Reserve University, Cleveland, Ohio 44109-1998.

^cPresent address: West Michigan Cancer Center, Kalamazoo, Michigan 49007.

¹F. M. Khan, W. Sewchand, J. Lee, and J. F. Williamson, "Revision of tissue-maximum ratio and scatter maximum ratio concepts for cobalt 60 and higher energy x-ray beams," *Med. Phys.* **7**, 230–237 (1980).

²M. Tatcher and B. E. Bjarnagard, "Head-scatter factors in rectangular photon fields," *Med. Phys.* **20**, 205–206 (1993).

³J. J. M. van Gasteren, S. Heukelom, H. J. van Kleffens, R. van der Laarse, J. L. M. Venselaar, and C. F. Westermann, "The determination of phantom and collimator scatter components of the output of megavoltage photon beams: Measurement of the collimator scatter part with a beam coaxial narrow cylindrical phantom," *Radiother. Oncol.* **20**, 250–257 (1991).

⁴G. Krithivas and S. N. Rao, "Dosimetry of 24-MV x rays from a linear accelerator," *Med. Phys.* **14**, 274–281 (1987).

- ⁵K. R. Kase and G. K. Svensson, "Head-scatter data for several linear accelerators (4–18 MV)," *Med. Phys.* **13**, 530–532 (1986).
- ⁶G. Luxton and M. A. Astrahan, "Output factor constituents of a high energy photon beam," *Med. Phys.* **15**, 88–91 (1988).
- ⁷P. B. Dunscombe and J. M. Nieminen, "On the field size dependence of relative output from a linear accelerator," *Med. Phys.* **19**, 1441–1444 (1992).
- ⁸B. R. Thomadsen, "The use of tissue-air ratio with high energy photon fields," Dissertation, University of Wisconsin-Madison, Madison, Wisconsin, May, 1989.
- ⁹P. A. Jursinic and T. R. Mackie, "Characteristics of secondary electrons produced by 6-, 10-, and 24-MV photon beams" (submitted to *Medical Physics*).
- ¹⁰B. R. Thomadsen, S. Kubsad, B. R. Paliwal, S. Shahabi, and T. R. Mackie, "On the cause of the variation in tissue-maximum-ratio values with source to detector distance," *Med. Phys.* **20**, 723–727 (1993).
- ¹¹P. J. Biggs and M. D. Russel, "An investigation into the presence of secondary electrons in megavoltage photon beams," *Phys. Med. Biol.* **28**, 1033–1043 (1983).
- ¹²P. J. Biggs and C. C. Ling, "Electrons as the cause of the observed d_{\max} shift with field size in high energy photon beams," *Med. Phys.* **6**, 291–295 (1979).
- ¹³C. C. Ling, M. C. Schell, and S. N. Rustgi, "Magnetic analysis of the radiation components of a 10-MV photon beam," *Med. Phys.* **9**, 20–26 (1982).